KSCE Journal of Civil Engineering (2017) 21(5):1866-1881

DOI 10.1007/s12205-016-0962-y

Structural Engineering

pISSN 1226-7988, eISSN 1976-3808
www.springer.com/12205

Aerodynamic Stability Parameters Optimization and Global Sensitivity Analysis for a Cable Stayed Bridge

Nazim Abdul Nariman*

Received May 13, 2016/Revised July 16, 2016/Accepted August 08, 2016/Published Online October 7, 2016

Abstract

Cable stayed Bridges are highly vulnerable to strong wind load induced vibrations which are responsible of generating aerodynamic instability and in a critical situation lead to structural failure. This paper focuses on buffeting response and flutter instability in a cable stayed Bridge. A strong fluctuating wind is assigned to a cable stayed Bridge model in ABAQUS FE program to onset optimization and global sensitivity analysis through considering three aerodynamic parameters (wind attack angle, deck streamlined length and stay cables viscous damping) by targeting the vertical and torsional vibrations of the deck. The numerical simulations results in conjunction with the frequency analysis results emphasized the existence of such vibrations. Model validation performed by comparing the results of lift and moment coefficients between the present FE model and two benchmarks from the literature (flat plate theory and flat plate by Xavier *et al.*, 2015), which resulted in good agreements between them. Optimum values of the adopted aerodynamic parameters have been identified and discussed. Global sensitivity analysis based on Monte Carlo sampling method was utilized to formulate the surrogate models and the sensitivity indices so that to identify rational effect and role of each parameter on the aerodynamic stability of the structure.

Keywords: *aerodynamic stability, wind attack angle, streamlined section, viscous damping, flat plate theory, monte carlo, global sensitivity analysis*

1. Introduction

The safety and serviceability of long span cable supported bridges are often critical due to wind induced vibrations. Aerostatic and aerodynamic effects are two aspects of this type of vibration (Thiesemann *et al.*, 2003; Soon Duck, 2010; Mohammadi, 2013; You-Lin, 2013). The greatest aerodynamic effect is caused by flutter and the aerostatic effect is originated to the structural shape and the wind attack angle (Starossek, 1998; Selvam and Govindaswamy, 2001; Al-Assaf, 2006; Dorian, 2010; Keerthana *et al*., 2011; Ming Hui *et al*., 2012). Three types of responses are categorized in cable stayed bridges, global mode, local mode and coupled mode. The global mode is associated with the deformations of the deck-pylons system and the quasi-static motions of the stay cables; the local mode is often related to the motions of the stay cables only; the coupled mode has essential donations of both the deck- pylons system and stay cables (Ming-Yi and Pao-Hsii, 2012; Ubertini, 2008; Xu *et al*., 2014; Diana *et al*., 1998). Usually the pylons are rigidly designed, and there are no significant pylons deformations occur at lower modes of vibrations due to associated and nearby wind excitations. Thus, the coupled mode is the dominant which is resulting from the deck-stay cables interaction, where the effect of the pylons can be ignored (Chen *et al.*, 2001; Van Vu *et al.*, 2011; Odden and Skyvulstad, 2012). Long span bridges are exposed to lateral bending due to drag force, vertical bending due to lift force and torsional bending due to pitch moment. The buffeting responses of the long span bridges increase and become more notable when the increasing the Bridgespan and the deck width (Simiu and Scanlan, 1996; Xiang *et al.*, 2005; Kvamstad, 2011). The internal forces and the displacements resulted from buffeting responses are growing more apparent when the wind speed is high. As a result many serious effects are arising such as fatigue of the structural components of the cable stayed long span bridges.

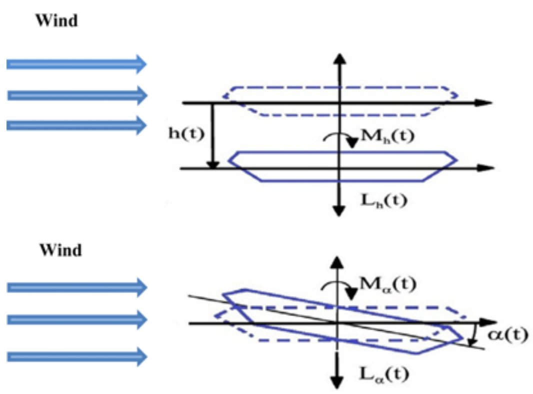

Fig.1. Vertical and Torsional Motions of the Deck

*Ph.D. Candidate, Institute of Structural Mechanics, Faculty of Civil Engineering, Bauahaus Universitat Weimar, 99423, Weimar, Germany (Corresponding Author, E-mail: nazim.nariman@uni-weimar.de)

Fig. 1. shows only the vertical and the torsional motions of a Bridgedeck due to buffeting, where these two types of motions are the axis of this study.

Three main factors are considered to be the basic supports for the buffeting responses of long span bridges, the intensity of the wind turbulence, the natural frequencies and the shape of the structure (Xiao *et al*., 2012; Chunhua and Haifan, 2000), where long span bridges with low natural frequencies or small deck widths are particularly exposed to flutter instability. The combination of buffeting and flutter can be the cause of large aerodynamic instabilities because of high vibrations amplitude. These aerodynamic instabilities generate negative aerodynamic damping and rapidly building up severe torsional and vertical vibrations resulting in the collapse of the structure shortly. The safety of the cable supported long span bridges usually is not related to buffeting, but it just causes discomfort for the users of these type of structures and fatigue of the structural elements (Chowdhury, 2004; Stærdahl *et al*., 2008; Shuxian, 2009). Particular care should be dedicated to flutter, where one of the main issues of the designers of long span cable supported bridges is the collapse possibility due to tragic flutter. Efficient and adequate information are needed for the probability of failure because of flutter, as it was the reason of failure in Tacoma narrow Bridgein 1940. The critical wind speed resulted in this accident was 42 mph. This critical wind speed resulted in vertical motion which was the reason of developing tardiness between the opposite sides of the Bridge providing a side to side twisting motion.

The aerodynamic stability and modification of long span cable stayed Bridge is necessary to be sophisticated (Matsumoto *et al*., 1995; Diana *et al*., 1998). Up to date understanding of bridge aerodynamic behavior and improved response prediction is a must to investigate the aerodynamic stability plans. Various analytical inspections regarding flutter and buffeting problems can be recognized (Bleich, 1948; Davenport, 1962; Scanlan, 1977; Lin and Yang, 1983; Xie and Xiang, 1985; Miyata and Yamada, 1988; Agar, 1989; Matsumoto *et al.*, 1994; Pfeil and Batista, 1995; Matsumoto and Chen, 1996; Jain *et al.,* 1996; Katsuchi *et al.*, 1999). The importance of coupling between the modes of vibration in the case of estimating the buffeting response, especially at situations of higher wind speeds is an important task, and the coupling between flutter and buffeting issues has been classified (Matsumoto *et al*., 1994; Jain *et al.*, 1996; Wilde and Fujino, 1998; Katsuchi *et al*., 1999). Several cases of analytical outputs of multimode flutter analyses of long span cable supported bridges mark the complicated aerodynamic coupling due to nearly spaced natural frequencies and 3D mode shapes. Moreover, flutter multimode coupling is not always originated by symmetric torsional mode (Miyata and Yamada, 1988; Agar, 1989; Chen, 2004; Yao-Jun and Hai-Fan, 2008).

Computational methods (Amiri *et al*., 2014a, b; Anitescu *et al*., 2015; Areias and Rabczuk, 2013; Areias *et al*., 2013a, b; Areias *et al*., 2014; Areias *et al.*, 2016; Bordas *et al*., 2008; Budarapu *et al.,* 2014a, b; Budarapu *et al.*, 2015a, b; Chauh-Dinh *et al.*, 2012; Ghorashi *et al.,* 2015; Nanthakumar *et al*., 2015; Nguyen-Thanh *et al.,* 2008; Nguyen-Thanh *et al.*, 2011; Nguyen-Thanh, 2015; Nguyen-Xuan, 2008; Phan-Dao *et al*., 2013; Rabczuk *et al.*, 2003; Rabczuk *et al.*, 2004a, b, c, d, e, f; Rabczuk and Belytschko, 2005; Rabczuk *et al.*, 2005; Rabczuk and Belytschko, 2006; Rabczuk and Eibl, 2006; Rabczuk and Belytschko, 2007; Rabczuk and Zi, 2007; Rabczuk *et al*., 2007a, b, c, d; Rabczuk and Samaniego, 2008; Rabczuk *et al.*, 2010a, b, c, d; Thai *et al.*, 2012; Thai *et al.*, 2014; Thai *et al.*, 2015; Valizadeh *et al.*, 2013; Valizadeh *et al*., 2015; Vu Bac *et al.*, 2016; Yang *et al.*, 2015; Zhuang *et al.*, 2014; Zi *et al.*, 2007) are well suited to complement experimental testing.

(Ma *et al.*, 2010) investigated the aerodynamic behavior of the Sutong bridge. They presented the main results of wind tunnel tests on a sectional model and the full aeroelastic models of the Sutong bridge. They discovered that both the lift and moment coefficients are increasing from (-1 to 0.5) and (-0.2 to 0.1) respectively with the increase of the turbulent wind attack angle between (-10° to 10°).

(Xavier *et al*., 2015) studied experimentally the effect of wind attack angle on the generation of lift and drag forces and pitching moment in a flat plate with multiple aspect ratios excited by a turbulent wind in the wind tunnel test. The results of the lift and the moment coefficients were supported on the range of wind attack angle between (0 to 90°). The lift coefficient and moment coefficient values were (-0.12 to 0.01) and (-0.01 to 0.01) respectively, which is an indicator that increasing the wind attack angle will increase the generated lift force and moment in the flat plate.

(Abdel-Aziz and Attia, 2015) conducted numerical analysis on four Bridge deck sections using a ANSYS software, they calculated the effect of wind attack angle on the lift and moment coefficients for the Bridge deck section. The range of turbulent wind attack angle was between (-10° to 10°), in the other hand the calculated lift coefficient was (-0.65 to 0.2) and the calculated moment coefficient was (-0.065 to 0.1). The results affirm the increase of lift force and pitching moment in the Bridge deck model.

In order to enhance the aerodynamic stability of long span bridges, it is necessary to study important aerodynamic parameters that are related to the source of buffeting which is the fluctuating wind, and to propose deck cross sections that are aerodynamically efficient to prevent vertical and torsional vibrations especially vibrations that are sourced by the coupled mode. Wherefore, it is largely essential to study the effect and the role of three parameters that are directly considered the source of the aerodynamic stability of the long span bridge. Hence, in this paper, finite element models of cable stayed Bridges are created using ABAQUS program to undergo strong wind excitations. Three aerodynamic parameters (wind attack angle, deck streamlined length and stay cables viscous damping) are dedicated for optimization process. Frequency analysis is utilized to recognize the type of vibrations for the cable stayed Bridge model. Global sensitivity analysis is conducted to formulate the surrogate models and identify the roles and the rational effects of each parameter on the buffeting response and the flutter instability of the structure.

2. Aerodynamic Stability Parameters

2.1 Wind Attack Angle

Two types of wind flow, laminar and turbulent are both the cases of dynamic vibration in long span cable stayed bridges. The cause of buffeting is due to unsteady wind loading on the structure because of speed fluctuation of the oncoming wind. Wind turbulence is a strong factor that affects the aerodynamic behavior of the structure (Haan, 2000; Bartoli *et al.*, 2008; Chen *et al.,* 2009; Xu *et al.*, 2014; Zhang *et al*., 2016). Bridge decks are subjected to large amplitudes of vibration because of turbulent high speed winds, in which large fluctuation of immediate angle of attack may result in aerodynamic nonlinearities that are considered to be critical for the safety of the structure. To model both buffeting and flutter vibrations, considering the effects of prompt angle of attack is a must, where this factor is obviously the source of high buffeting responses of the long span cable supported bridges (Ding *et al.*, 2000; Diana, 1998).

2.2 Deck Section

Due to increase in the length of the Bridge span, these types of structures are turning more flexible, consequently this property entails the study of bluff body aerodynamics regarding the flutter instability of the Bridge deck. The shapes of Bridge decks have complex cross sections, so wind tunnel test is an important solution to define the aerodynamic derivatives, and it is largely important to select efficient deck models to avoid flutter instability (Scanlan, 1977; Bartoli *et al*., 2008; Hernandez *et al*., 2012).

Bluff bodies, such as Bridge decks are aerodynamically classified into three section types basing on the characteristics of the wind flow created supporting on zero angle of wind attack (Fransos, 2008; Dahl, 2013).

2.3 Viscous Damping of Stay Cables

The stay cables are considered the main structural elements of long span cable stayed bridges. Due to flexible, relative small mass and highly low damping, stay cables are exposed to large amplitude vibrations by wind excitation. These vibrations can be the cause of stay cables fatigue and eventual decrease of their service life, Soltane *et al*., 2010. The sag of a stay cable occurs with a catenary shape because of its weight and tensile force.The sagging of the stay cables should be considered when a single straight cable element is used to represent the stay cable. The tensile stiffness of the stay cable is assumed to be elastically ideal. Furthermore, the bending stiffness, compressive and shear stiffness are negligible. The nonlinearity of the cable sagging can be simulated supporting on the stay cable equivalent modulus of elasticity (see Eq. (1)).

$$\boldsymbol{E_{eq}} = \frac{\boldsymbol{E_c}}{\mathbf{1} + \frac{(\boldsymbol{wl_c})^2 \boldsymbol{A_c E_c}}{\mathbf{12}\boldsymbol{T}^3}} \tag{1}$$

where E_c, A_c and l_c are the effective modulus of elasticity, the cross-sectional area and the horizontal projected length of the stay cable, respectively; w is the weight of the stay cable per unit length; T is the tension in the stay cable. In global analysis of cable stayed bridges, one common practice is to model each cable as a single truss element with an equivalent modulus to allow for sag (Sardesai and Desai, 2013). The element stiffness matrix in local coordinates for such a cable element can be written as:

$$\boldsymbol{k_c} = \frac{\boldsymbol{A_c E_{eq}}}{\boldsymbol{l_c}} \begin{bmatrix} \mathbf{1} & \mathbf{0} & \mathbf{-1} & \mathbf{0} \\ \mathbf{0} & \mathbf{0} & \mathbf{0} & \mathbf{0} \\ \mathbf{-1} & \mathbf{0} & \mathbf{1} & \mathbf{0} \\ \mathbf{0} & \mathbf{0} & \mathbf{0} & \mathbf{0} \end{bmatrix} \tag{2}$$

Under the excitation of a wind, the stay cable vibrates due to energy dissipation results in damping effect of the stay cables. It is a fact that the damping of a stay cable is too low (0.005-0.01) and its vibration cannot be avoided. Hence, instruments such as viscous dampers with certain characteristics could be used to mitigate the vibration.

3. Equation of Motion

The effect of flutter implicates nonlinear aerodynamic behavior, so it has been plausible in many examples to deal with the problem as linear analytical methods. Whereas the justification for this deal is that structural response is generally treated as linear elastic and following exponentially modification of the sinusoidal oscillation. The separation between the stable and the unstable systems is conducted by a primary condition that may be treated as to have small amplitude to start it, (Simiu and Scanlan, 1996). The equation of motion of a cable stayed Bridge subjected to wind excitations, referred to the global coordinate system, can be stated in a matrix form as follows:

$$\boldsymbol{M\ddot{D}(t)} + \boldsymbol{C\dot{D}(t)} + \boldsymbol{KD(t)} = \boldsymbol{F^s(t)} + \boldsymbol{F^b(t)} \tag{3}$$

where $\mathbf{D(t)}$: is the nodal displacement vector, $\mathbf{\dot{D}(t)}$ and $\mathbf{\ddot{D}(t)}$ are the vectors of the nodal velocity and acceleration, respectively. $\mathbf{M}$, $\mathbf{C}$ and $\mathbf{K}$ are the matrices of mass, damping and stiffness, respectively, $\mathbf{F^s}$ is the self-excited force vector, $\mathbf{F^b}$ is the buffeting force vector. In the flutter analysis, the buffeting force is not included in Eq. (3) because flutter is related to the aerodynamic damping and stiffness that are induced by the self-excited force only (Chen *et al.*, 2000; Chen, 2006; Chen, 2012).

3.1 Aerodynamic Forces and Moment

The vibration of Bridge deck generally implicates torsional deformation of the deck, and a relevant excitation technique for which there is a solution which is a direct analysis. Aerodynamic forces are coupling together vertical and torsional natural modes of vibrations. Flat plate theory is used a s a base for the analytical solution, where this provides good results even for many practical box girder deck sections, such as Severn Bridge which is the frontier example. The forces per unit length ***Fx*** and ***Fy*** along the fixed body axes (x-axis and y-axis respectively) are computed using the measured pressures. The mean force coefficients in x and y directions are obtained as given below:

$$\overline{\mathbf{C}}_{Fx} = \frac{\overline{\mathbf{F}}_x}{\mathbf{B}\left(\frac{1}{2}\rho\overline{\mathbf{U}}_z^2\right)} \tag{4}$$

$$\overline{\mathbf{C}}_{\mathbf{Fy}} = \frac{\overline{F}_y}{\mathbf{B}\left(\frac{1}{2}\rho\overline{\mathbf{U}}_z^2\right)} \tag{5}$$

where $\overline{\mathbf{C}}_{\mathbf{Fx}}$ and $\overline{\mathbf{C}}_{\mathbf{Fy}}$ are mean force coefficient along x and y axes and **B** is the characteristic dimension which is taken as the height of the Bridge section. The resultant of the aerodynamic forces experienced by a structure subjected to wind action can be resolved into drag ***FD***, (along- wind) force acting in the direction of the mean wind and lift ***FL***, (across- wind) force acting perpendicular to the direction of the mean wind. By resolving ***Fx*** and ***Fy*** in the direction of wind and perpendicular to the direction of wind, the drag force ***FD*** and the lift force ***FL***, respectively are obtained. Forces along drag and lift directions are computed based on the equations given below (Ricciardelli 2002 and Nelson 2011):

$$\overline{\mathbf{C}}_{\mathbf{D}} = \frac{\overline{\mathbf{F}}_{\mathbf{D}}}{\mathbf{0.5}\rho\overline{\mathbf{U}}_z^2\mathbf{B}} \tag{6}$$

$$\overline{\mathbf{C}}_{\mathbf{L}} = \frac{\overline{\mathbf{F}}_{\mathbf{L}}}{\mathbf{0.5}\rho\overline{\mathbf{U}}_z^2\mathbf{B}} \tag{7}$$

The wind induced moments are the effects resulting from the normal forces on the Bridge surface at top and bottom multiplied by their lever arms and integrated over the entire surface. Moment coefficient is computed from:

$$\overline{\mathbf{C}}_{\mathbf{M}} = \frac{\overline{\mathbf{M}}}{0.5\rho\overline{\mathbf{U}}_z^2\mathbf{B}^2} \tag{8}$$

where $\overline{\mathbf{C}}_{\mathbf{D}}$, $\overline{\mathbf{C}}_{\mathbf{L}}$ and $\overline{\mathbf{C}}_{\mathbf{M}}$ are mean drag, lift force and moment coefficients, respectively, $\mathbf{0.5}\rho\overline{\mathbf{U}}_z^2$ is the reference pressure at deck height z, due to mean wind speed $\overline{\mathbf{U}}$ and ρ is the density of air (Ge and Xiang, 2009).

4. Finite Element Model

A cable stayed Bridge model is created in ABAQUS with 324 m length and 22 m width, the main parts of the Bridge is the deck which consists of connected reinforced concrete deck segments with 2.6 m height. Four reinforced concrete pylons with square shapes 4 × 4 m dimensions and 103 m height, and 80 stay cables are connecting the deck to the pylons in a fan shape arrangement, each cable with cross section area 0.00785 m^2. The main steel bar diameter is 0.06 m and the diameter of the temperature steel bars in addition to the stirrups are 0.04 m. The boundary condition of the deck is fixed in one side and free for longitudinal translation in the other side. The pylons are fixed at the bottom and each two pylons are connected by six reinforced concrete ties with 4 × 4 m dimensions and 22 m length. The stay cables equivalent Young's modulus of elasticity has been used to approximate the sagging occurrence in the cables because it was modeled as truss elements (see Table 1).

Table 1. Material Properties

Material	Mass Density Kg/m^3	Young's Modulus of Elasticity Pa	Poisson's ratio
High strength concrete	2643	3.10E+10	0.25
Steel bar	7800	2.00E+11	0.30
Stay cable	9438	1.65E+11	0.30

The deck is modeled as (C3D10: A10-quadratic tetrahedron) elements, pylons and ties are modeled as (C3D8R: An 8 node linear brick reduced integration hourglass control) elements, the reinforcing steel bars are modeled as (B31: A 2-node linear beam in space) elements and the stay cables are modeled as (T3D2: A 2- node linear 3D truss) elements.

4.1 Mesh Convergence

Sufficiently refined mesh is important to make sure that the results obtained from ABAQUS simulations are suitable. Coarse meshes can yield inaccurate results in analyses using implicit or explicit methods. The numerical solutions of the models will tend toward a unique value as the mesh is refined. The mesh will be converged when additional mesh refinement produces a negligible change in the results. Mesh convergence was performed supporting on the results of the natural frequencies for eight mode shapes of vibrations. A uniform mesh refinement was considered with equal element size for each element type, where the results are calculated 14 times (see Fig. 2).

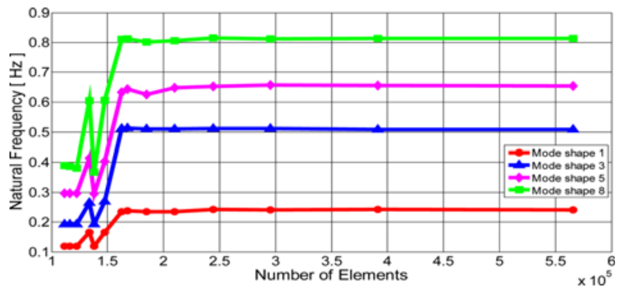

Fig. 2. Mesh Convergence Considering four Mode Shapes of Vibrations

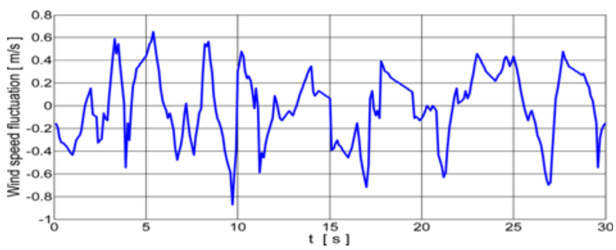

Fig. 3. Wind Speed Fluctuation Time History

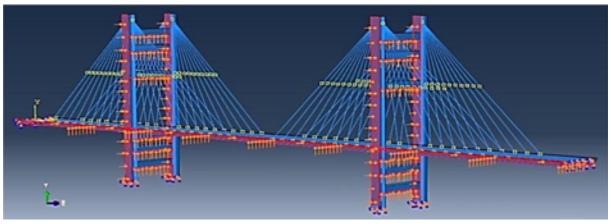

Fig. 4. Wind Pressure Assignation to the Model

The mesh convergence obviously starts with constant path approximately from 250000 elements. To create the model of the cable stayed Bridge, the total of 391577 elements were used consisting of (10872-C3D8R elements, 108125-C3D10 elements, 6088-T3D2 elements and 266492-B31elements) which falls in the convergence region with finer mesh size.

4.2 Wind Load

A strong wind with design speed of 47 m/sec has been dedicated in the numerical simulations, and the frequency of the excitation is arranged to produce a frequency falls in the frequency ranges of first eight mode shapes of vibrations of the cable stayed Bridge model so that to include the vertical and torsional modes. The wind pressure assigned in the simulations is with duration of 30 seconds (see Fig. 3). The wind fluctuation data has been prepared depending on exact data from the literature in addition to modification of the excitation frequency (Hao *et al*., 2010).

The cable stayed Bridge model is divided into five regions over its height by taking in account the wind pressure variation due to elevation from the ground. The wind pressure is designed to excite the cable stayed Bridge model perpendicular to the longitudinal axis without skewedness. The wind forces (lift and drag) and moment are assigned to the cable stayed Bridge regions as pressure values supporting on the level of each region along the height (see Fig. 4).

4.3 Frequency Analysis

To analyze the predicted types of vibrations of the cable stayed

Table 2. Mode Shapes and Frequencies

Mode shape	Type	Eigenvalue	Frequency (Hz)
1	Vertical	2.311	0.242
2	Vertical	4.764	0.347
3	Vertical	10.248	0.509
4	Vertical	14.842	0.613
5	Lateral – Torsional	16.941	0.655
6	Vertical – Torsional	23.817	0.776
7	Torsional	24.612	0.789
8	Vertical	26.131	0.813

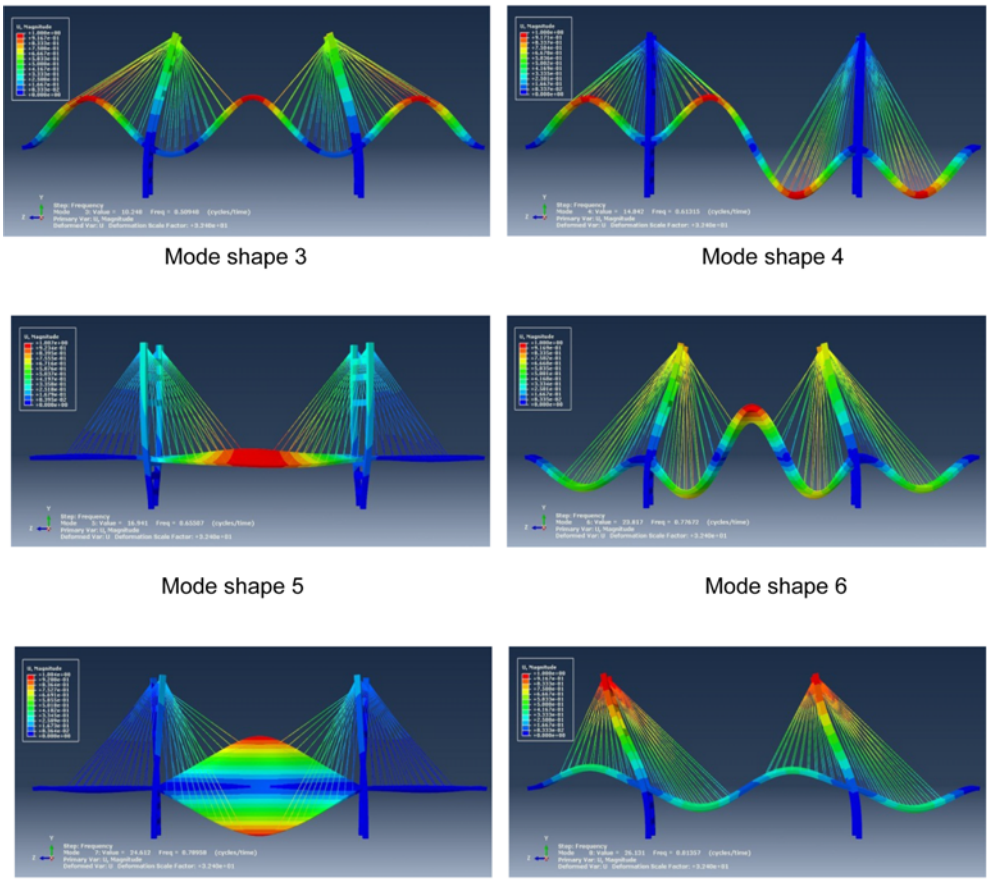

Mode shape 3 Mode shape 4

Mode shape 5 Mode shape 6

Mode shape 7 Mode shape 8

Fig. 5. Eight Mode Shapes of Vibrations (Frequency Analysis)

Bridge model, frequency analysis is conducted using ABAQUS FE program. The mode shapes of vibrations are being calculated so that to identify the dominant mode shapes of vibrations and to confirm the occurrence of vertical and torsional vibrations in the deck. The mode shapes of vibrations with low frequencies are more prone to occur than the rest mode shapes with high frequencies due to the nature of the actual winds except the situations of strong winds.

4.3.1 Results of mode shapes

The first 8 mode shapes of vibrations have been obtained, the type of vibration and the related frequency were determined for each mode shape. The first 4 mode shapes are vertical vibrations modes and their frequencies are 0.242 Hz, 0.347 Hz, 0.509 Hz and 0.613 Hz respectively (see Table 2).

The fifth and sixth mode shapes are coupled lateral torsional and vertical torsional vibrations with frequencies 0.655 Hz and 0.776 Hz respectively. While in the seventh and eighth mode shapes are torsional and vertical vibrations respectively.

4.3.2 Simulation of the Mode Shapes

The screen shots of the eight mode shapes of the cable stayed Bridge model frequency analysis in Fig. 5 are simulating the type of the predicted vibrations that can be expected for the wind excitation. The displacements are shown obviously and the colors are representing the magnitude of the displacements in each point on the cable stayed Bridge structure. The scale factor has been magnified automatically by ABAQUS so that to thoroughly express on the type of vibrations and their effect on the structural response.

4.4 Aerodynamic Instability Analysis

A strong wind excitation on the cable stayed Bridge is modeled with duration of 30 seconds. The selected case for the aerodynamic parameters is the situation where the wind attack angle value is 30°, the deck streamlined length is 1.14 m and the stay cables viscous damping is 0.0086 N.s/m. Numerical simulation is conducted for this model and data are collected for the buffeting response and flutter instability of the structural model.

4.4.1 Results of Vertical Vibrations

The vertical displacements at the mid span center of the deck are varying with time during 30 seconds of the numerical simulation. The first 7 seconds, the displacements do not exceed 0.008 m, but after that region the deck starts to vibrate stronger, and the vertical displacement of the deck reaches 0.03 cm (see Fig. 6). This is an indication that the vertical buffeting deck response exists and the frequency of the vibration is 0.5 Hz approximately calculated using the graph of the vertical displacement time history of the deck center to calculate the number of the cycles per time. As a result it is realized that the third vertical mode shape of vibration is dominant in this case where the natural frequency of this mode is 0.509 Hz.

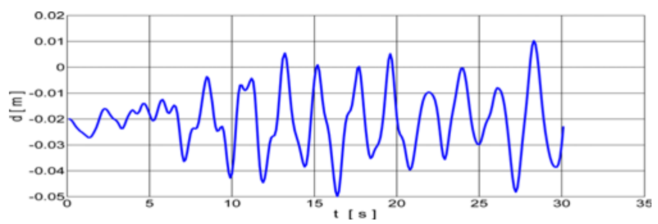

Fig. 6. Time History of Vertical Vibration at Mid-span Center of the Deck

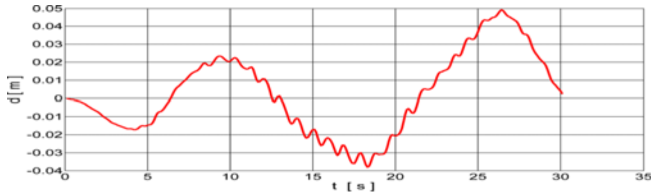

Fig. 7. Time History of Torsional Vibration at Mid-span Outer Edges of the Deck

4.4.2 Results of Torsional Vibrations

The torsional displacements at the mid span outer edges of the deck are varying with time during 30 seconds of the numerical simulation. The first 8 seconds, the displacements do not exceed 0.023 m which means that flutter is not obvious, but after that area the deck starts to flutter rapidly every 1 second with a maximum torsional displacement of 0.05 m till 27 seconds of the numerical simulation (see Fig. 7). This is an indication that the torsional flutter of the deck exists and the frequency of the vibration is 0.72 Hz approximately calculated using the graph of the vertical displacement time history of the deck left edge to calculate the number of the cycles per time. This certifies that the sixth coupled vertical-torsional mode shape of vibration is dominant in this case where the natural frequency of this mode is 0.776 Hz.

4.4.3 Simulation of Aerodynamic Instability

To confirm the existence of aerodynamic instability in the cable stayed Bridge model excited by a strong wind, the following eight screen shots of numerical simulation which have been detailed in previous section, are being discussed (see Fig. 8).

The first screen shot at time 9 seconds shows the generation of torsional vibration in the middle part of the deck only, where the colors are indicating this fact due to graduation of colors in one edge only. The second screen shot at time 11.8 second displays the additional generation of torsional vibration in the left and right parts of the deck. The third screen shot at time 12 second indicates the occurrence of vertical vibration in the left part (regular distribution of color) beside the torsional vibration of the center part of the deck. The fourth screen shot at time 12.4 second proofs the generation of vertical vibration of the center part of the deck only (regular distribution of the color). The fifth screen shot at time 12.9 seconds exhibits the generation of vertical vibration at the left part of the deck. The sixth screen shot at time 14.4 seconds shows up occurrence of torsional

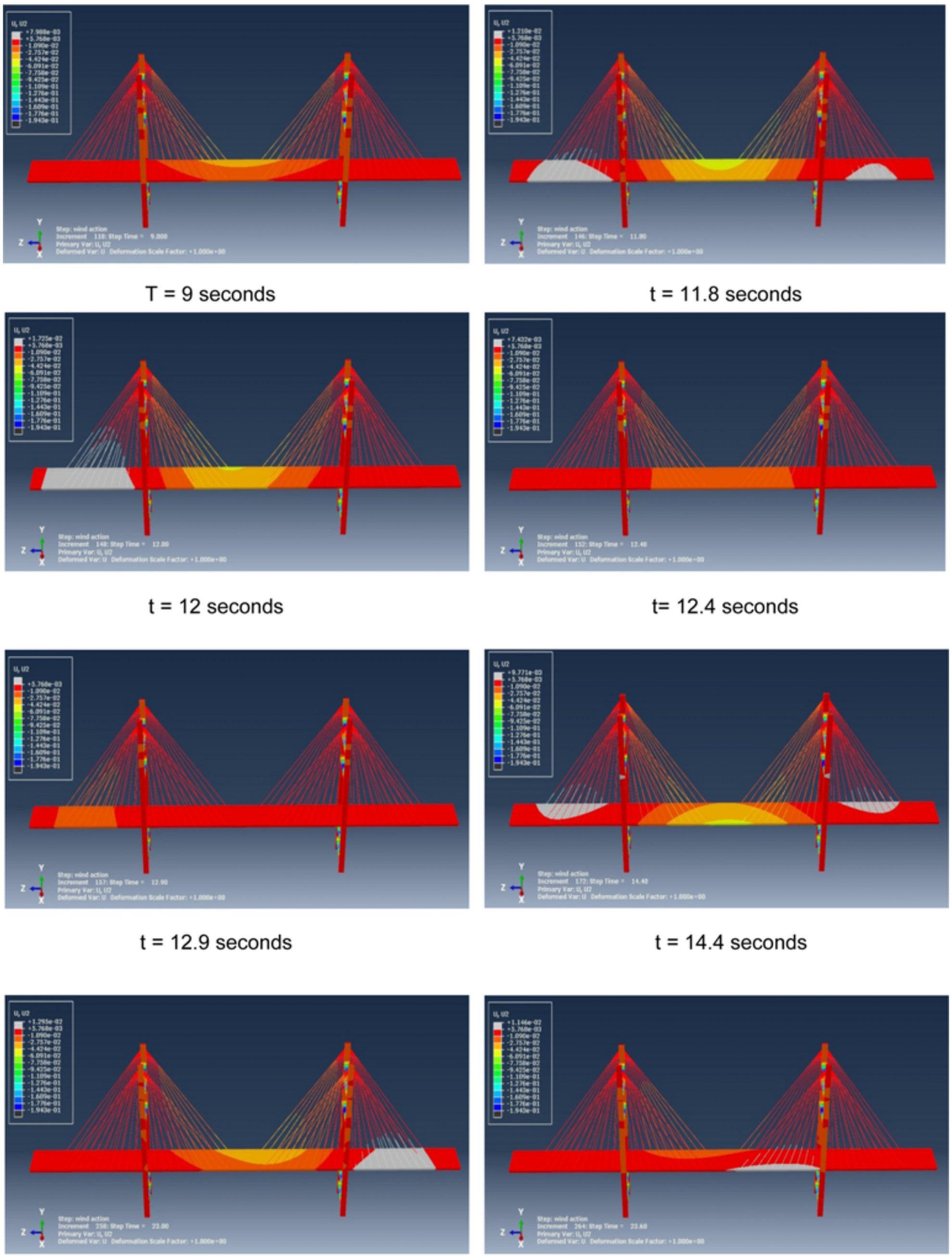

T = 9 seconds   t = 11.8 seconds

t = 12 seconds   t= 12.4 seconds

t = 12.9 seconds   t = 14.4 seconds

t = 23 seconds   t = 23.6 seconds

Fig. 8. Six Screen Shots of Vibration in the Cable Stayed Bridge Model

vibrations in all parts of the deck like the situation of the second screen shot but in the opposite side. The seventh screen shot at time 23 seconds features the generation of torsional vibration in the center part and vertical vibration in right part of the deck like the third screen shot but in the opposite side. Finally the eighth screen shot at time 23.6 seconds reveals the occurrence of a different torsional vibration between the right and left sides of the center part of the deck. This is a firm fact on that the buffeting vertical response and the flutter torsional instability of the deck pour into the fact of existence of aerodynamic instability of the cable stayed Bridge due to strong wind excitation.

Table 3. Aerodynamic Parameters and Range Values

Aerodynamic parameter	First value	Second value	Third value
Wind attack angle (°)	0	22.5	45
Deck streamlined length (m)	0	1	2
Stay cables viscous damping (N.s /m)	0.005	0.0075	0.01

5. Aerodynamic Parameters Optimization

Three aerodynamic parameters are utilized to realize their effects on the vertical vibration and the torsional vibration of the deck in a cable stayed Bridge model. Optimization of these parameters is conducted to identify the optimum values that are taking part in the aerodynamic stability of the cable stayed bridge, this by decreasing both the buffeting response and the flutter instability of the structure. The first aerodynamic parameter (wind attack angle) is the source of fluctuation of wind excitation that generates the buffeting response in the cable stayed Bridge directly, and the second aerodynamic parameter (deck streamlined length) is responsible of the generation of both vertical and torsional vibration of the deck due to vortex shedding incidence, and the third aerodynamic parameter (stay cables viscous damping) is related to the control of the stay cables oscillation which takes part in the aerodynamic stability of the cable stayed bridge. Table 3 shows the range values of each aerodynamic parameter.

In order to evaluate the effects of the three aerodynamic parameters on the vertical and torsional vibrations of deck, nine models are utilized for the optimization process. Three cases for each aerodynamic parameter are considered, and ABAQUS numerical simulations are being adopted for the wind excitation on the cable stayed Bridge model for a duration of 30 seconds.

5.1 Results of Wind Attack Angle Effect

When increasing the wind attack angle parameter in the FE model three times, starting from 0°, 22.5° and 45°, the displacement at the center of the deck mid-span will increase in a linear way approximately to higher values. The effect of this parameter starts to appear from the beginning of the wind excitation and continues in the same pattern till the end of the 30 seconds of the numerical simulation, where the maximum displacement at the center of the deck mid span reaches 0.04 m after 16 seconds for the wind attack angle of 45° and for wind attack angle 22.5° reaches 0.03 m, but for wind attack angle 0° is 0.02 m (see Fig. 9).

This behavior means that increasing the wind attack angle will increase the vertical vibration of the deck. While increasing this

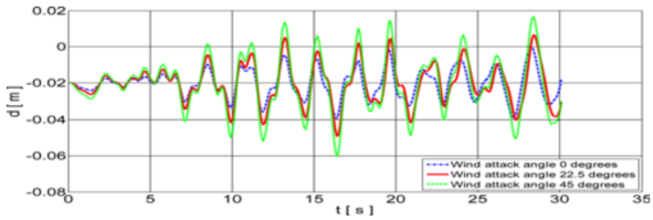

Fig. 9. Wind Attack Angle Effect on the Displacement at Deck Mid-span

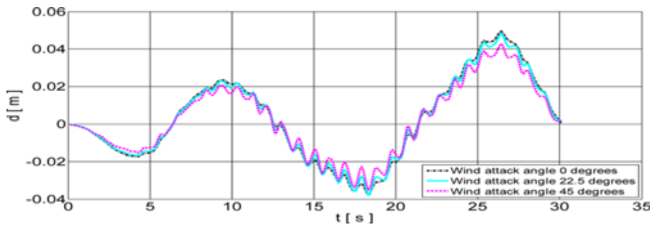

Fig. 10. Wind Attack Angle Effect on the Displacement at Deck Mid-span

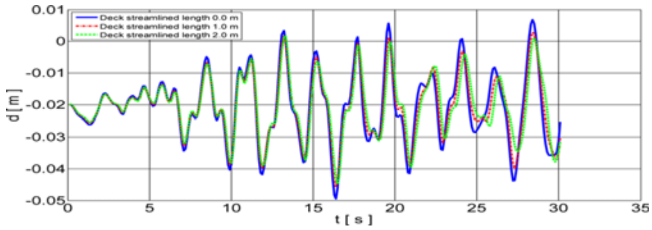

Fig. 11. Deck Streamlined Length Effect on the Displacement at Deck Mid-span

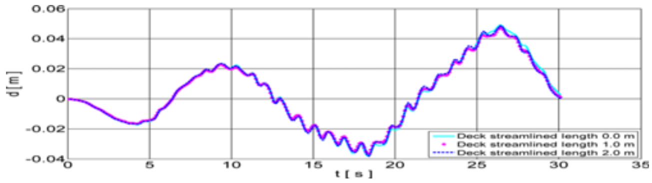

Fig. 12. Deck Streamlined Length Effect on the Displacement at Deck Mid-span

parameter from 0°, 22.5°and 45° will increase the flutter displacement of the deck reaching to 0.042 m for wind attack angle 45° and reaches 0.05 m both for wind attack angles 22.5° and 0° after 27 seconds of the wind excitation. The speed of repeated fluttering of the deck starts obviously after 8 seconds and continues till 27 seconds of the numerical simulation and the speed of the flutter occurrence increases with the increase of the wind attack angle (see Fig. 10).

5.2 Results of Deck Streamlined Length Effect

Increasing the deck streamlined length parameter in the FE model three times, starting from 0.0 m, 1.0 m and 2.0 m, the displacement at the center of the deck mid-span will decrease to lower values. The effect of this parameter starts to appear after 7 seconds of the wind excitation and continues in the same pattern till the end of the 30 seconds of the numerical simulation. The maximum displacement at the center of the deck mid span reaches 0.0275 m after 28 seconds for the deck streamlined length of 0.0 m and for deck streamlined length 1.0 m reaches 0.0225 m, but for deck streamlined length 2.0 m is 0.02 m (see Fig. 11).

This is an indication that adopting streamlined sections for the deck will decrease the vertical vibration of the deck. While increasing this parameter from 0.0 m, 1.0 m and 2.0 m will have a very small non appreciable effect on the flutter displacement of the deck reaching to 0.05 m for all cases approximately after 27 seconds of the wind excitation. The speed of repeated fluttering of the deck starts obviously when after 8 seconds and continues till 27 seconds of the numerical simulation as for wind attack angle cases, and the speed of the flutter occurrence stays stable when increasing the deck streamlined length (see Fig. 12).

5.3 Results of Stay Cables Viscous Damping Effect

This time when increasing the stay cables viscous damping in the FE model three times, starting from 0.005, 0.0075 and 0.01, the displacement at the center of the deck mid-span will decrease

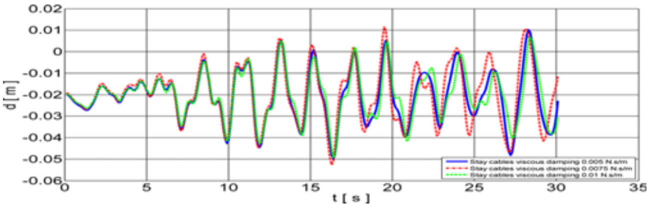

Fig. 13. Viscous Damping of Stay Cables Effect on the Displacement at the Center of the Deck Mid-span

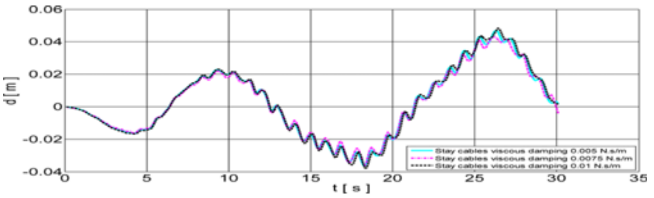

Fig. 14. Viscous Damping of Stay Cables Effect on the Displacement at the Outer Edges of the Deck Mid-span

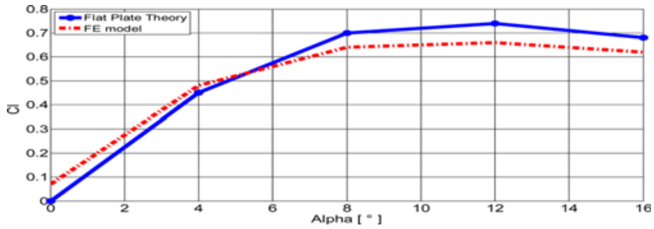

Fig. 15. Lift Coefficient C_L with Wind Attack Angle Validation

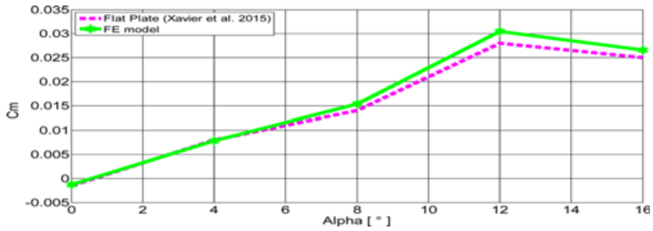

Fig. 16. Moment Coefficient C_m with Wind Attack Angle Validation

in a small range with irregular pattern. The effect of this parameter starts to appear after 6 seconds of the wind excitation and continues in the different patterns from a stable to increasing and decreasing again during the 30 seconds of the numerical simulation. The maximum displacement at the center of the deck mid span reaches 0.032 after 19 seconds for the stay cables viscous damping of 0.0075 N.s/m and for stay cables viscous damping 0.005 N.s/m reaches 0.025, but for stay cables viscous damping 0.01 N.s/m is 0.025 too (see Fig. 13). A nonlinear behavior exists due to variation of the stay cables viscous damping values in relation with the vertical vibrations of the deck. Considering torsional vibration of the deck, when increasing this parameter from 0.005, 0.0075 and 0.01 will have a very small non appreciable effect on the flutter displacement of the deck for all cases but just for a period of time between 23-28 seconds reaching to maximum 0.0475 m for both 0.005 and 0.01 cases approximately and becomes 0.0425 m for 0.0075 case. The speed of repeated fluttering of the deck starts obviously after 8 seconds and continues till 27 seconds of the numerical simulation, and the speed of the flutter occurrence increases with the increase of the stay cables viscous damping (see Fig. 14).

6. Model Validation

The lift and moment coefficients calculated for the ABAQUS FE deck model are validated with two benchmarks from the latest literature. First benchmark is the results obtained from the flat plate theory and the second benchmark is the results of the flat plate model collected from experiments done by (Xavier *et al*., 2015). Table 4 shows the data of the lift coefficient C_L and moment coefficient C_M for the two benchmarks and the numerical analysis results calculated from the ABAQUS FE model.

Table 4. Results of Lift and Moment Coefficients for ABAQUS FE Model and Two Benchmarks

	FE model	Flat Plate Theory	FE model	Flat Plate (Xavier)
Angle of attack	C_L	C_L	C_M	C_M
0°	0.070	0.000	-0.0013	-0.0015
4°	0.480	0.450	0.0078	0.0080
8°	0.640	0.700	0.0154	0.0140
12°	0.660	0.740	0.0305	0.0280
16°	0.620	0.680	0.0266	0.0250

6.1 Lift Coefficient Validation

There is a very good agreement between the results of the lift coefficient C_L for the FE model and the flat plate theory in relation with multiple wind attack angle cases as shown in Fig. 15, where the curves of the data for the two approaches are in a coinciding pattern starting from 0°-16° of wind attack angle. There is a small difference in lift coefficient value between them which is not exceeding 0.1 for the maximum situation for the wind attack angle of 12°.

6.2 Moment Coefficient Validation

The comparison between the results of the moment coefficient C_M for the FE model and the results of the flat plate model experiment done by (Xavier *et al.*, 2015) for the wind attack angle cases is pointing to a good agreement between them. The two curves are coinciding to a good extent in the range of 0°-16° of wind attach angle and the maximum difference in moment coefficient is 0.0025 at the situation of 12° wind attach angle (see Fig. 16).

7. Sensitivity Analysis

Sensitivity analysis is the study of how the uncertainty in the output of the model can be handed out to various sources of input, or it attributes to the identification of individual donation and various origins of uncertain inputs to the uncertainty in the output of a model (Saltelli *et al*., 2000; Saltelli, 2004; Saltelli *et* *al.*, 2008; Keitel *et al.*, 2011). There are two sorts of sensitivity analysis methods: local and global sensitivity analysis. Local sensitivity analysis methods calculate or convergent the local response of the model outputs through modifying input parameters or individual parameters with other parameters at nominal values in the hyperspace of the input parameter. In the other hand, global sensitivity analysis estimates the effects of input variations on the outputs in the total permitted ranges of the input space (Confalonieri *et al.*, 2010; Tong, 2010; Che-Sheng *et a*l., 2013; Baroni and Tarantola, 2014).

The probability distributions of **X1**, **X2** and **X3** which are wind attack angle, deck streamlined length and the stay cables viscous damping respectively have been assumed to be normal or Gaussian distributions and have been accomplished using MATLAB codes so that to use them to construct the sample based on Monte Carlo sampling method. The aerodynamic parameters **X1**, **X2** and **X3** are arranged in samples according to the Monte Carlo sampling method. These samples are used to determine the predicted vertical and torsional displacements both at the center and outer edges of the deck mid-span respectively, so that to formulate the surrogate models for upcoming sensitivity analysis.

7.1 Sobol's Sensitivity Indices

Sobol's indices are a global sensitivity measures which determine the contribution of each parameter (or group of parameters) to the variance of the output. The usual Sobol sensitivity indices include the main and total effects for each parameter, but the method can also provide specific interaction terms (Glen and Isaacs, 2012). It uses a variance ratio to estimate the importance of parameters. This method is based on the partitioning of the total variance of model output **V(Y)** using the following equation:

$$\mathbf{V(Y)} = \sum_{i=1}^{n} \mathbf{V_i} + \sum_{i\le j\le n}^{n} \mathbf{V_{ij}} \ldots + \sum_{i\le \ldots n}^{n} \mathbf{V_{1\ldots n}} \tag{9}$$

where $\mathbf{V_1}$ represent the first order effect for each parameter $\mathbf{X_i(V_i\text{-}V[E(Y|X_i)])}$ and: $\mathbf{V_{ij}} = \mathbf{V(E(Y|X_i, X_j)) - V_i - V_j}$ to $\mathbf{V_{1\ldots \mathit{n}}}$ the interactions among n parameters. The first-order sensitivity index S_i can be calculated by:

$$\mathbf{S_i} = \frac{\mathbf{V_i}}{\mathbf{V(Y)}} - \frac{\mathbf{V[E(Y|X_i)]}}{\mathbf{V(Y)}} \tag{10}$$

where $\mathbf{V[E(Y|X_i)]}$ is the variance of the expected value of **Y** when conditioning with respect to $\mathbf{X_i}$, and **V(Y)** is the unconditional variance of **Y**. And the second-order sensitivity index $\mathbf{S_{ij}}$ can be calculated by:

$$\mathbf{S_{ij}} = \frac{\mathbf{V_{ij}}}{\mathbf{V(Y)}} - \frac{\mathbf{V[E(Y|X_i, X_j)] - V_i - V_j}}{\mathbf{V(Y)}} \tag{11}$$

In general, the total sensitivity index $\mathbf{S_{Ti}}$ can be defined as (Homma and Saltelli, 1996; Saltelli and Tarantola, 2002; Saltelli and Annoni, 2010):

$$\mathbf{S_{Ti}} = \frac{\mathbf{E(V(Y|X_{\sim i}))}}{\mathbf{V(Y)}} \tag{12}$$

where the subscript **~i** refers to all of the inputs except input **i**, Also the total sensitivity index $\mathbf{S_{Ti}}$ can be written as:

$$\mathbf{S_{Ti}} = \mathbf{1} - \frac{\mathbf{V(E(Y|X_{\sim i}))}}{\mathbf{V(Y)}} \tag{13}$$

where $\mathbf{V(E(Y|X_{\sim i}))}$ is the variance of the expected value of **Y** when conditioning with respect to all parameters except for $\mathbf{X_i}$. Due to parameter interaction $\mathbf{S_{Ti}}$ of a parameter increases, therefore $\Sigma\mathbf{S_{Ti}} \ge 1$ will always hold. The difference $\mathbf{S_{Ti} - S_i}$ is a measure of how much $\mathbf{X_i}$ interacts with other input parameters. The index $\mathbf{S_i}$ is therefore a measure of the exclusive influence of input parameter $\mathbf{X_i}$ If the sum of all $\mathbf{S_i}$ is close to one, the model is additive with respect to its variances and no remarkable interactions between the parameters seem to exist.

7.2 Results and Discussion of the Surrogate Models

The regression coefficients calculated both for vertical and torsional actual displacements supported on Monte Carlo experimental method, and in order to formulate the surrogate models for the predicted vertical and torsional displacements, 400 samples were used considering convergence process between the sensitivity indices. Quadratic and interaction terms are used to construct he surrogate model for the case of vertical displacement at the center of the deck mid-span. The calculated coefficient of determination R^2 between the actual and the predicted vertical displacements was 98.12% (see Fig. 17) which is an excellent representation of the predicted vertical displacement, which means that just 1.88% of the system response still unexplained.

Quadratic and interaction terms are used to build the surrogate model to calculate the torsional displacement at the outer edges of the deck mid-span. The coefficient of determination R^2 calculated between the actual and the predicted torsional displacements was 97.50% which is a very good approximation for the prediction of torsional displacement that only 2.50% of the system response

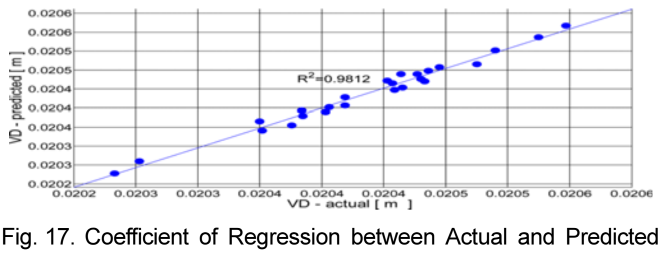

Fig. 17. Coefficient of Regression between Actual and Predicted Vertical Displacement

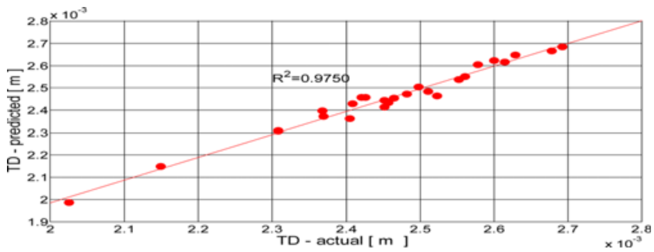

Fig. 18. Coefficient of Regression between Actual and Predicted Torsional Displacement

Table 5. Sensitivity Indices of the Aerodynamic Parameters

Sensitivity indices	Vertical displacement	Torsional displacement
First order **X1**	0.682520	0.557385
First order **X2**	0.154241	0.236873
First order **X3**	0.129080	0.205698
Sum of first orders	**0.965841**	**0.999956**
Interaction between **X1** and **X2**	0.011241	0.000107
Interaction between **X1** and **X3**	0.008712	0.000044
Interaction between **X2**and **X3**	0.000537	0.000082
Total order of **X1**	0.702473	0.557536
Total order of **X2**	0.166019	0.237062
Total order of **X3**	0.138329	0.205824
Sum of total orders	1.006821	1.000422

remains unexplained (see Fig. 18).

7.3 Results and Discussion of Sensitivity Indices

The main orders of sensitivity indices for each aerodynamic parameter in addition to their interaction orders were calculated considering the convergence results which recommended using 400 samples to calculate both the vertical displacement and torsional displacement at the center and the outer edges of the mid span of the cable stayed Bridge model respectively (see Fig. 19 and Fig. 20). Supporting on the calculated results, the total sensitivity indices for each aerodynamic parameter have been calculated (see Table 5).

In relation with the vertical displacement, the total order sensitivity index of aerodynamic parameter (wind attack angle) is 0.7024, this value is bigger than the total order sensitivity index of aerodynamic parameter (deck streamlined length) **X2** which is 0.1660, also it is bigger than the total order sensitivity index of aerodynamic parameter (stay cables viscous damping) **X3** which is 0.1383, this means that the vertical displacement is 70.24% due to variation in the wind attack angle, and it is 16.60% due to the variation in the deck streamlined length. Also it is 13.83% due to the variation in the stay cables viscous damping. While the interaction index between the aerodynamic parameters **X1** and **X2** is 0.0112 and between **X1** and **X3** is 0.0087, while between **X2** and **X3** is 0.0005, which means that there is a small interaction between the aerodynamic factors taking part in the variation of the vertical displacement of the deck at the center of the mid span.

While considering the torsional displacement , the total order sensitivity index of **X1** is 0.5575, which is the biggest aerodynamic parameter which is bigger twice of the total order sensitivity index of **X2** which is 0.2370 approximately, also it is bigger twice the total order sensitivity index of **X3** which is 0.2058 approximately, this means that the torsional displacement is dependable 55.75% on the wind attack angle variation, while it is 23.70% due to the deck streamlined length variation, and it is 20.58% due to the variation in stay cables viscous damping. While the interaction index between **X1** and **X2** is 0.0001 and between **X1** and **X3** is 0.0000, in the other hand, between **X2** and **X3** is 0.0000 too, this proofs that the surrogate model is additive

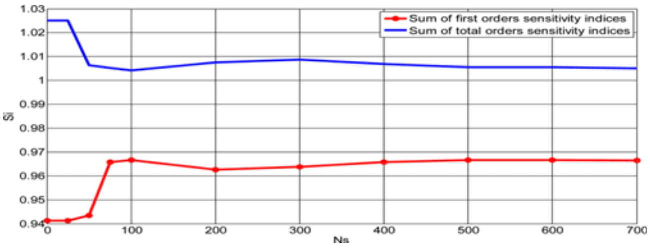

Fig. 19. Convergence of Sensitivity Indices –vertical Displacement

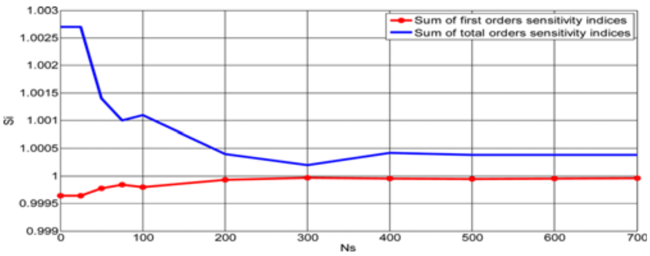

Fig. 20. Convergence of Sensitivity Indices –torsional Vibration

approximately which means that there is no interaction between aerodynamic parameters take part in the variation of the torsional displacement of the deck at the outer edges of the mid span.

7.4 Convergence of the Results

The process of global sensitivity analysis supporting on Sobol's sensitivity indices requires certain or adequate samples of experiments to find out the predicted effect of the aerodynamic parameters on the response of the system. The most efficient number of samples is being identified through the convergence of the sum of first orders and total sensitivity indices of the aerodynamic parameters. All the sensitivity indices (first orders, interaction orders and total orders) for each aerodynamic parameter have been calculated using m MATLAB codes. Two outputs have been utilized in the process of converges, the vertical displacement and torsional displacement. Fig. 19 and Fig. 20 show the relation between the number of samples and the sum of first orders sensitivity indices, in the same time between the number of samples and the sum of total sensitivity indices of the three aerodynamic parameters. For the case of vertical displacement (see Fig. 19), the two curves of the sum of first orders and total orders of sensitivity indices at the beginning are not coinciding to reach convergence till 400 samples. After this stage the two curves are starting to converge at the 400 number of samples, where the two curves continue to remain in a stable position after many times of changing the number of samples.

Also for the torsional displacement (see Fig. 20) the two curves are reaching convergence at 400 samples too, and the coinciding pattern continues.

The convergence results of the two cases necessitate utilizing 400 samples of experiments to efficiently get the predicted rational effects of each aerodynamic parameter on both the variation of the vertical displacement and torsional displacement.

8. Conclusions

The following points have been concluded:

1. The numerical simulations in conjunction with frequency analysis confirmed the existence of vertical and torsional vibrations of the deck due to wind excitation which is being considered as a basic reference to understand the buffeting response and flutter instability of the cable stayed Bridge in the design stage and after construction.
2. Three aerodynamic parameters have been optimally identified their values that are responsible of improving the aerodynamic instability of the cable stayed Bridge and to skip improper designs before construction stage and enhance the serviceability and safety of the structure against vibrations hazards.
3. Global sensitivity analysis of the aerodynamic parameters formulated surrogate models which are utilized to predict the buffeting response and flutter instability of the cable stayed Bridge so that to dedicate suitable plans and solutions for each vibration case thoroughly.
4. The sensitivity indices revealed the rational effect and role of each aerodynamic parameter on the aerodynamic instability of the structure which are considered important data to identify the priorities in the design procedure so that to optimize the response of the system against vertical and torsional vibrations of the deck which are resulting due to strong critical wind excitations.

Acknowledgements

The author wishes to thank and express his gratitude to Prof. Dr.-Ing. Timon Rabczuk, the chair of computational mechanics at Bauhaus Universität-Weimar, for his continuous support and invaluable assistance in providing guidance and consultancy relating to this research paper.

References

Abdel-Aziz, A. and Attia, W. A. (2015). "Aeroelastic investigation of different deck sections for suspension bridges by numerical analysis." *International Journal of Engineering and Innovative Technology (IJEIT)*, Vol. 4, No. 12, pp. 49-57, DOI: http://www.ijeit.com/Vol%204/Issue%2012/IJEIT1412201506_09.pdf.

Agar, T. J. A. (1989). "Aerodynamic flutter analysis of suspension bridges by a modal technique." *Engrg. Struct.*, Vol. 11, No. 2, pp. 75-82, DOI: 10.1016/0141-0296(89)90016-3.

Al-Assaf, A. (2006). *Flutter analysis of open-truss stiffened suspension bridges using synthesized aerodynamic derivatives*, PhD Thesis, Washington State University, Department of Civil and Environmental Engineering, Washington, USA.

Amiri, F., Anitescu, C., Arroyo, M., Bordas, S., and Rabczuk, T. (2014)." XLME interpolants, a seamless bridge between XFEM and enriched meshless methods." *Computational Mechanics*, Vol. 53, No. 1, pp. 45-57, DOI: 10.1007/s00466-013-0891-2.

Amiri, F., Milan, D., Shen, Y., Rabczuk, T., and Arroyo, M. (2014). "Phase-field modeling of fracture in linear thin shells." *Theoretical and Applied Fracture Mechanics*, Vol. 69, pp. 102-109, DOI: 10.1016/j.tafmec.2013.12.002.

Anitescu, C., Jia, Y., Zhang, Y., and Rabczuk, T. (2015). "An isogeometric collocation method using superconvergent points." *Computer Methods in Applied Mechanics and Engineering*, Vol. 284, pp. 1073-1097, DOI: 10.1016/j.cma.2014.11.038.

Areias, P. and Rabczuk, T. (2013). "Finite strain fracture of plates and shells with configurational forces and edge rotation." *International Journal for Numerical Methods in Engineering*, Vol. 94, No. 12, pp. 1099-1122, DOI: 10.1002/nme.4477.

Areias, P., Msekh, M. A., and Rabczuk, T. (2016)." Damage and fracture algorithm using the screened Poisson equation and local remeshing." *Engineering Fracture Mechanics*, Vol. 158, pp. 116-143, DOI: 10.1016/j.engfracmech.2015.10.042.

Areias, P., Rabczuk, T., and Camanho, P. P. (2013). "Initially rigid cohesive laws and fracture based on edge rotations." *Computational Mechanics*, Vol. 52, No. 4, pp. 931-947, DOI: 10.1007/s00466-013-0855-6.

Areias, P., Rabczuk, T., and Dias-da-Costa, D. (2013)." Element-wise fracture algorithm based on rotation of edges." *Engineering Fracture Mechanics*, Vol. 110, pp. 113-137, DOI: 10.1016/j.engfracmech.2013.06.006.

Areias, P. M. A., Rabczuk, T., and Camanho, P. P. (2014). "Finite strain fracture of 2D problems with injected anisotropic softening elements." *Theoretical and Applied Fracture Mechanics*, Vol. 72, pp. 50-63, DOI: 10.1016/j.tafmec.2014.06.006.

Baroni, G. and Tarantola, S. (2014). "A general probabilistic framework for uncertainty and global sensitivity analysis of deterministic models: A hydrological case study." *Environmental Modelling & Software*, Vol. 51, pp. 26-34, DOI: 10.1016/j.envsoft.2013.09.022.

Bartoli, G., Asdia, P., Febo, S., Pasto, C., and Procino, L. (2008). *Innovative solutions for long-span suspension Bridges,* BBAA VI International Colloquium on: Bluff Bodies Aerodynamics and Applications. Milano, Italy, 16 pages.

Bleich, F. (1948). "Dynamic instability of truss-stiffened suspension bridges under wind action." *Proc. ASCE*, Vol. 74, No. 7, pp. 1269-1314.

Bordas, S., Rabczuk, T., and Zi, G. (2008). "Three-dimensional crack initiation, propagation, branching and junction in non-linear materials by extrinsic discontinuous enrichment of meshfree methods without asymptotic enrichment." *Engineering Fracture Mechanics*, Vol. 75, No. 5, pp. 943-960, DOI: 10092/705.

Budarapu, P. R., Gracie, R., Bordas, S. P. A., and Rabczuk, T. (2014). "An adaptive multiscale method for quasi-static crack growth." *Computational Mechanics*, Vol. 53, No. 6, pp. 1129-1148, DOI: 10.1007/s00466-013-0952-6.

Budarapu, P. R., Gracie, R., Yang, S. W., Zhaung, X., and Rabczuk, T. (2014). "Efficient coarse graining in multiscale modeling of fracture." *Theoretical and Applied Fracture Mechanics*, Vol. 69, pp. 126-143, DOI: 10.1016/j.tafmec.2013.12.004.

Budarapu, P. R., Javvaji, B., Sutrakar, V. K., Mahapatra, D. R., Zi, G., and Rabczuk, T. (2015). "Crack propagation in Graphene." *Journal of Applied Physics*, Vol. 118, No. 064307, DOI: 10.1063/1.4928316.

Budarapu, P. R., Narayana, T. S. S., Rammohan, B., and Rabczuk, T. (2015). "Directionality of sound radiation from rectangular panels." *Applied Acoustics*, Vol. 89, pp. 128-140, DOI: 10.1016/j.apacoust.2014.09.006.

Budarapu, P. R., SudhirSastry, Y. B., and Natarajan, R. (2016). "Design concepts of an aircraft wing: Composite and morphing airfoil with auxetic structures." *Frontiers of Structural and Civil Engineering*, accepted for publication.

Budarapu, P. R., SudhirSastry, Y. B., Javvaji, B., and Mahapatra, D. R. (2014). "Vibration analysis of multi-walled carbon nanotubes embedded in elastic medium." *Frontiers of Structural and Civil Engineering*, Vol. 8, No. 2, pp. 151-159, DOI: 10.1007/s11709-014-0247-9.

Cai, Y., Zhu, H., and Zhuang, X. (2014). "A Continuous/discontinuous Deformation Analysis (CDDA) method based on deformable blocks for fracture modelling." *Frontiers of Structural & Civil Engineering*, Vol. 7, pp. 369-378, DOI: 10.1007/s11709-013-0222-x.

Chau-Dinh, T., Zi, G., Lee, P. S., Rabczuk, T., and Song, J. H. (2012). "Phantom-node method for shell models with arbitrary cracks." *Computers & Structures*, Vol. 92-93, pp. 242-256, DOI: 10.1016/j.compstruc.2011.10.021.

Che-Sheng, Z., Xiao-Mong, S., Jun, X., and Charles, T. (2013). "An efficient integrated approach for global sensitivity analysis of hydrological model parameters." *Environmental Modelling & Software*, Vol. 41, pp. 39-52, DOI: 10.1016/j.envsoft.2012.10.009.

Chen Suren (2004). *Dynamic performance of bridges and vehicles under strong wind*, PhD Thesis, Department of Civil and Environmental Engineering, Louisiana State University, Louisiana, USA.

Chen, X. (2006). "Analysis of long span bridge response to winds: building nexus between flutter and buffeting." *Journal of Structural Engineering*, Vol. 132, No. 12, pp. 2006-2017, DOI: 10.1061/(ASCE)0733-9445(2006)132:12(2006).

Chen, X. (2012). "Prediction of buffeting response of long span bridges to transient non stationary winds." *The Seventh International Colloquium on Bluff Body Aerodynamics and Applications (BBAA7)*, Shanghai, China.

Chen, X., Kareema, A., and Matsumoto, M. (2001). "Multimode coupled flutter and buffeting analysis of long span bridges." *Journal of Wind Engineering and Industrial Aerodynamics*, Vol. 89, pp. 649-664, DOI: 10.1016/S0167-6105(01)00064-2.

Chen, Z. Q., Han, Y., Hua, X. G., and Luo, Y. Z. (2009). "Investigation on influence factors of buffeting response of bridges and its aeroelastic model verification for Xiaoguan Bridge." *Engineering Structures*, Vol. 31, No. 2, pp. 417-431, DOI: 10.1016/j.engstruct.2008.08.016.

Chen, S. R., Cai, C. S., Chang, C. C., and Gu, M. (2004). "Modal coupling assessment and approximated prediction of coupled multimode wind vibration of long-span bridges." *Journal of Wind Engineering and Industrial Aerodynamics*, Vol. 92, pp. 393-412, DOI: 10.1016/j.jweia.2004.01.004.

Chen, X., Matsumoto, M., and Kareem, A. (2000). "Aerodynamic coupling effects on flutter and buffeting of bridges." *J. of Engineering Mechanics*, ASCE, Vol. 126, No. 1, pp. 17-26, DOI: 10.1061/(ASCE)0733-9399(2000)126:1(17).

Chowdhury, A. G. (2004). *Identification of frequency domain and time domain aeroelastic parameters for flutter analysis of flexible structures*, PhD Thesis, Iowa State University, Department of Aerospace Engineering, Iowa, USA.

Chunhua, L. and Haifan, X. (2000). "Simulation of buffeting response history for long span bridges." *8th ASCE Specialty Conference on Probabilistic Mechanics and Structural Reliability*, Notre Dame, Indiana.

Confalonieri, R. , Bregaglio, S., and Acutis, M. (2010). "A proposal of an indicator for quantifying model robustness based on the relationship between variability of errors and of explored conditions." *Ecological Modelling*, Vol. 221, pp. 960-964, DOI: 10.1016/j.ecolmodel.2009.12.003.

Dahl, K. (2013). *Aeroelastic behavior of very long span suspension bridges*, MSc thesis, University of Stavanger, Department of Structural Engineering and Materials Science, Stavanger, Norway.

Davenport, A. G. (1962). "Buffeting of a suspension bridge by storm winds." *Journal of the Structural Division*, ASCE, Vol. 88, No. 3, pp. 233-270, DOI: http://cedb.asce.org/CEDBsearch/record.jsp?dockey=0012826.

Diana, G., Bruni, S., Collina, A., and Zasso, A. (1998). "Aerodynamic challenges in super long span bridges design." *Bridge aerodynamics*, Larsen and Esdahl, eds., pp. 131-144, DOI: 10.5169/seals-59842.

Ding, Q, Lee, P. K. K., and Lo, S. H. (2000). " Time domain buffeting analysis of suspension bridges subjected to turbulent wind with effective attack angle." *Journal of Sound and Vibration*, Vol. 233, No. 2, pp. 311-327, DOI: 10.1006/jsvi.1999.2801.

Dorian, J. (2010). *Aspects of wind buffeting response and non-linear structural analysis for cable stayed Bridges*, TDV Consulting GmbH, Dorian Janjic & Partner, Graz, Austria.

Fransos, D. (2008). *Stochastic numerical models for wind engineering*, PhD thesis. Polytechnic University of Turin, Torino, Italy.

Ge, Y. J. and Xiang, H. F. (2009). "Aerodynamic stabilization for box-girder suspension bridges with super-long span. EACWE 5." Florence, Italy.

Ghorashi, S., Valizadeh, N., Mohammadi, S., and Rabczuk, T. (2015). "T-spline based XIGA for fracture analysis of orthotropic media." *Computers & Structures*, Vol. 147, pp. 138-146, DOI: 10.1016/j.compstruc.2014.09.017.

Glen, G. and Isaacs, K. (2012). "Estimating Sobol sensitivity indices using correlations." *Journal of Environmental Modelling and Software*, Vol. 37, pp. 157-166, DOI: 10.1016/j.envsoft. 2012.03.014.

Haan, F. L. (2000). *The effects of turbulence on the aerodynamics of long span bridges*, PhD Thesis, University of Notre Dame, Department of Aerospace and Mechanical Engineering, Notre Dame, Indiana.

Hao, W., Aiqun, L., Gengwen, Z., and Jian, L. (2010). "Non-linear buffeting response analysis of long-span suspension bridges with central buckle." *Earthquake Engineering and Engineering Vibration*, Vol. 9, No. 2, pp. 259-270, DOI: 10.1007/s11803-010-0011-7.

Hernández, S., Nieto, F., Jurado, J. A., and Pérez, I. (2012). "Bluff body aerodynamics of simplified bridge decks for aeroelastic optimization." *The Seventh International Colloquium on Bluff Body Aerodynamics and Applications (BBAA7),* Shanghai, China.

Hollerud Odden, T. and Skyvulstad, H. (2012). *Wind-induced Dynamic Response and Aeroelastic Stability of a Suspension Bridge crossing Sognefjorden*, MSc Dissertation, Norwegian University of Science and Technology, Department of Structural Engineering. Trondhiem, Norway.

Homma, T. and Saltelli, A. (1996). "Importance measures in global sensitivity analysis of model output." *Reliability Engineering and System Safety*, Vol. 52, No. 1, pp. 1-17, DOI: 10.1016/0951-8320(96)00002-6.

Jain, A., Jones, N. P., and Scanlan, R. H. (1996). "Coupled flutter and buffeting analysis of long-span bridges." *Journal of Structural Engineering.*, ASCE, Vol. 122, No. 7, pp. 716-725, DOI: 10.1061/(ASCE)0733-9445(1996)122:7(716).

Janjic, D. (2010). "Aspects of wind buffeting response and non-linear structural analysis for cable stayed bridges." *TDV Consulting GmbH, Dorian Janjic & Partner*, Graz, Austria.

Katsuchi, H., Jones, N. P., and Scanlan, R. H. (1999). "Multimode coupled flutter and buffeting analysis of the Akashi-Kaikyo Bridge." *Journal of Structural Engineering.*, ASCE, Vol. 125, No. 1, pp. 60-

70, DOI: 10.1061/(ASCE)0733-9445(1999)125:1(60).

Keerthana, M., Jaya, K. P., Selvi Rajan, S., Thampi, H., and Sankar, R. R. (2011). " Numerical studies on evaluation of aerodynamic force coefficients of cable-stayed bridge deck." *Journal of wind and Engineering*, Vol. 8, No. 2, pp. 19-29, DOI: https://www.researchgate.net/publication/267231443.

Keitel, H., Karaki, G., Lahmer, T., Nikulla, S., and Zabel, V. (2011). "Evaluation of coupled partial models in structural engineering using graph theory and sensitivity analysis." *Engineering structures*, Vol. 33, No. 12, pp. 3726-3736, DOI: 10.1016/j.engstruct.2011.08.009.

Kvamstad, T. H. (2011). *Assessment of the flutter stability limit of the Hålogaland Bridge using a probabilistic approach*. MSc thesis, Norwegian University of Science and Technology NTNU, Department of Structural Engineering, Trondheim, Norway.

Kwon, S. D. (2010). *Uncertainty of bridge flutter velocity measured at wind tunnel tests*. Chapel Hill, North Carolina, USA.

Lin, Y. K. and Yang, J. N. (1983). "Multi-mode bridge response to wind excitations." *Journal of Engineering Mechanics*, ASCE, Vol. 109, No. 2, pp. 586-603, DOI: 10.1061/(ASCE)0733-9399(1983)109:2(586).

Liu, M. Y. and Wang, P. H. (2012). "Finite element analysis of cable-stayed bridges with appropriate initial shapes under seismic excitations focusing on deck-stay interaction." *Department of Civil Engineering, Chung Yuan Christian University*, Jhongli city, Taiwan, Chap. 9, pp. 231-256, DOI: 10.5772/48440.

Ma, C. M., Liao, H. l., and Tao, Q. (2010). "Wind tunnel test on the wind-resistant behavior of a long-span cable-stayed bridge during erection." *Joumal of Southwest Jiaotong University,* Vol. 18, No. 2, pp. 112-117, DOI: 1005-2429(2010) 02-0112-06.

Matsumoto, M. and Chen, X. (1996). "Time domain analytical method of buffeting response for long span bridges." *Proc., 14th Nat. Symp. on Wind. Engrg., Japan Association for Wind Engineering*, pp. 515-520 (in Japanese).

Matsumoto, M., Chen, X., and Shiraishi, N. (1994). "Buffeting analysis of long span bridge with aerodynamic coupling." *Proc., 13th Nat. Symp. on Wind Engrg., Japan Association for Wind Engineering*, 227-232 (in Japanese).

Matsumoto, M., Niihara, Y., Kobayashi, Y., Shirato, H., and Hamasaki, H. (1995). "Flutter mechanism and its stabilization of bluff bodies." Proc., 9th ICW*E*, New Delhi, India, pp. 827-838.

Ming-Hui, H., Yuh-Yi, L., and Ming-Xi, W. (2012). "Flutter and buffeting analysis of bridges subjected to skew wind." *Journal of Applied Science and Engineering*, Vol. 15, No. 4, pp. 401-413, DOI: 10.6180%2fjase.2012.15.4.10.

Miyata, T. and Yamada, H. (1988). "Coupled flutter estimate of a suspension bridge." *Proc., Int. Colloquium on Bluff Body Aerodyn. And its Appl.*, Kyoto, pp. 485-492.

Mohammadi, M. S. (2013). *Wind Loads on Bridges Analysis of a three span bridge based on theoretical methods and Eurocode 1*. M.Sc dissertation. Royal Institute of Technology (KTH), Department of Civil and Architectural Engineering, Stockholm, Norway.

Nanthakumar, S., Valizadeh, N., Park, H., and Rabczuk, T. (2015)." Shape and topology optimization of nanostructures using a coupled XFEM/Level set method." *Computational Mechanics*, Vol. 56, No. 1, pp. 97-112, DOI: 10.1007/s00466-015-1159-9.

Nelson, S. R. (2011). *Experimental investigation of wind effects on long-span slender bridges with stochastic traffic flow*, M.Sc thesis. Colorado State University, Department of Civil and Environmental Engineering. Fort Collins, Colorado, USA.

Nguyen-Thanh, N., Kiendl, J., Nguyen-Xuan, H., Wuchner, R., Bletzinger, K. U., Bazilevs, Y., and Rabczuk, T. (2011). "Rotation free isogeometric thin shell analysis using PHT-splines." *Computer Methods in Applied Mechanics and Engineering*, Vol. 200, No. 47-48, pp. 3410-3424, DOI: 10.1016/j.cma.2011.08.014.

Nguyen-Thanh, N., Rabczuk, T., Nguyen-Xuan, H., and Bordas, S. (2008). "A smoothed finite element method for shell analysis." *Computer Methods in Applied Mechanics and Engineering*, Vol. 198, No. 2, pp. 165-177, DOI: 10.1016/j.cma.2008.05.029.

Nguyen-Thanh, N., Valizadeh, N., Nguyen, M. N., Nguyen-Xuan, H., Zhuang, X., Areias, P., Zi, G., Bazilevs, Y., De Lorenzis, L., and Rabczuk, T. (2015). "An extended isogeometric thin shell analysis based on Kirchho-Love theory." *Computer Methods in Applied Mechanics and Engineering*, Vol. 284, pp. 265-291, DOI: 10.1016/j.cma.2014.08.025.

Nguyen-Xuan, H., Rabczuk, T., Bordas, S., and Debongnie, J. F. (2008). "A smoothed finite element method for plate analysis." *Computer Methods in Applied Mechanics and Engineering*, Vol. 197, Nos. 13-16, pp. 1184-1203, DOI: 10.1016/j.cma.2007.10.008.

Pfeil, M. S. and Batista, R. C. (1995). "Aerodynamic stability analysis of cable-stayed bridges." *Journal of Structural Engineering*, ASCE, Vol. 121, No. 12, pp.1784-1788, DOI: 10.1061/(ASCE)0733-9445(1995)121:12(1784).

Phan-Dao, H., Nguyen-Xuan, H., Thai-Hoang, C., Nguyen-Thoi, T., and Rabczuk, T. (2013). "An edge-based smoothed finite element method for analysis of laminated composite plates." *International Journal of Computational Methods*, Vol. 10, No. 1, art. no. 1340005, DOI: 10.1142/S0219876213400057.

Rabczuk, T., Akkermann, J., and Eibl, J. (2005). "A numerical model for reinforced concrete structures." *International Journal of Solids and Structures*, Vol. 42, Nos. 5-6, pp. 1327-1354, DOI: 10.1016/j.ijsolstr.2004.07.019.

Rabczuk, T. and Belytschko, T. (2004). "Cracking particles: A simplified meshfree method for arbitrary evolving cracks." *International Journal for Numerical Methods in Engineering*, Vol. 61, No. 13, pp. 2316-2343, DOI: 10.1002/nme.1151.

Rabczuk, T. and Belytschko, T. (2005). "Adaptivity for structured meshfree particle methods in 2D and 3D." *International Journal for Numerical Methods in Engineering*, Vol. 63, No. 11, pp. 1559-1582, DOI: 10.1002/nme.1326.

Rabczuk, T. and Belytschko, T. (2006). "Application of particle methods to static fracture of reinforced concrete structures." *International Journal of Fracture*, Vol. 137, Nos. 1-4, pp.19-49, DOI: 10.1007/s10704-005-3075-z.

Rabczuk, T. and Belytschko, T. (2007). "A three dimensional large deformation meshfree method for arbitrary evolving cracks." *Computer Methods in Applied Mechanics and Engineering*, Vol. 196, Nos. 29-30, pp. 2777-2799, DOI: 10.1016/j.cma.2006.06.020.

Rabczuk, T., Belytschko, T., and Xiao, S. P. (2004). "Stable particle methods based on Lagrangian kernels." *Computer Methods in Applied Mechanics and Engineering*, Vol. 193, Nos. 12-14, pp. 1035-1063, DOI: 10.1016/j.cma.2003.12.005.

Rabczuk, T. and Eibl, J. (2004). " Numerical analysis of prestressed concrete beams using a coupled element free Galerkin finite element method." *International Journal of Solids and Structures*, Vol. 41 Nos. 3-4, pp. 1061-1080, DOI: 10.1016/j.ijsolstr.2003.09.040.

Rabczuk, T. and Eibl, J. (2006). "Modeling dynamic failure of concrete with meshfree particle methods." *International Journal of Impact Engineering*, Vol. 32, No. 11, pp. 1878-1897, DOI: 10092/139.

Rabczuk, T. and Samaniego, E. (2008). " Discontinuous modelling of shear bands using adaptive meshfree methods." *Computer Methods* *in Applied Mechanics and Engineering*, Vol. 197, Nos. 6-8, pp. 641-658, DOI: 10.1016/j.cma.2007.08.027.

Rabczuk, T. and Zi, G. (2007). "A meshfree method based on the local partition of unity for cohesive cracks." *Computational Mechanics*, Vol. 39, No. 6, pp. 743-760, DOI: 10.1007/s00466-006-0067-4.

Rabczuk, T., Areias, P. M. A., and Belytschko, T. (2007). "A simplied meshfree method for shear bands with cohesive surfaces." *International Journal for Numerical Methods in Engineering*, Vol. 69, No. 5, pp. 993-1021, DOI: 10.1002/nme.1797.

Rabczuk, T., Areias, P. M. A., and Belytschko, T. (2007). "A meshfree thin shell method for nonlinear dynamic fracture." *International Journal for Numerical Methods in Engineering*, Vol. 72, No. 5, pp. 524-548, DOI: 10.1002/nme.2013.

Rabczuk, T., Bordas, S., and Zi, G. (2010). "On three-dimensional modelling of crack growth using partition of unity methods." *Computers & Structures*, Vol. 88, Nos. 23-24, pp. 1391-1411, DOI: 10.1016/j.compstruc.2008.08.010.

Rabczuk, T., Bordas, S., and Zi, G. (2007). "A three-dimensional meshfree method for continuous multiplecrack initiation, nucleation and propagation in statics and dynamics." *Computational Mechanics*, Vol. 40, No. 3, pp. 473-495, DOI: 10.1007/s00466-006-0122-1.

Rabczuk, T., Eibl, J., and Stempniewski, L. (2003). "Simulation of high velocity concrete fragmentation using SPH/MLSPH." *International Journal for Numerical Methods in Engineering*, Vol. 56, No. 10, pp. 1421-1444, DOI: 10.1002/nme.617.

Rabczuk, T., Eibl, J., and Stempniewski, L. (2004). " Numerical analysis of high speed concrete fragmentation using a meshfree Lagrangian method." *Engineering Fracture Mechanics*, Vol. 71, pp. 547-556, DOI: 10.1016/S0013-7944(03)00032-8.

Rabczuk, T., Gracie, R., Song, J. H., and Belytschko, T. (2010). "Immersed particle method for fluid-structure interaction." *International Journal for Numerical Methods in Engineering*, Vol. 81, No. 1, pp. 48-71, DOI: 10.1002/nme.2670.

Rabczuk, T., Samaniego, E., and Belytschko, T. (2007). "Simplied model for predicting impulsive loads on submerged structures to account for fluid-structure interaction." *International Journal of Impact Engineering*, Vol. 34, No. 2, pp. 163-177, DOI: 10.1016/j.ijimpeng.2005.08.012.

Rabczuk, T., Zi, G., Bordas, S., and Nguyen-Xuan, H. (2010). "A geometrically non-linear three dimensional cohesive crack method for reinforced concrete structures." *Engineering Fracture Mechanics*, Vol. 75, No. 16, pp. 4740-4758, DOI: 10.1016/j.engfracmech.2008.06.019.

Rabczuk, T., Zi, G., Bordas, S., and Nguyen-Xuan, H. (2010). "A simple and robust three-dimensional cracking-particle method without enrichment." *Computer Methods in Applied Mechanics and Engineering*, Vol. 199, Nos. 37-40, pp. 2437-2455, DOI: 10.1016/j.cma.2010.03.031.

Ricciardelli, F. (2002). "Pressure distribution, aerodynamic forces and dynamic response of box sections." *Journal of Wind Engineering and Industrial Aerodynamics*, Vol. 90, No. 10, pp. 1135-1150, DOI: 10.1016/S0167-6105(02)00227-1 .

Saltelli, A. and Tarantola, S. (2002). "On the relative importance of input factors in mathematical models: Safety assessment for nuclear waste disposal." *Journal of American Statistical Association,* Vol.97, No. 459, pp. 702-709, DOI: http://www.jstor.org/stable/3085706.

Saltelli, A. and Paola Annoni (2010). "How to avoid a perfunctory sensitivity analysis." *Environmental Modelling and Software,* Vol. 25, No. 12, pp. 1508-1517, DOI: 10.1016/j.envsoft.2010.04.012.

Saltelli, A. K., Chan, K., and Scott, M. (2000). *Sensitivity Analysis*, New York, John Wiley & Sons publishers.

Saltelli, A., Ratto, M., Andres, T., Campolongo, F., Cariboni, J., and Gatelli, D. (2008). *Global Sensitivity Analysis: The Primer,* John Wiley & Sons Ltd.

Saltelli Andrea (2004). *Global sensitivity analysis: An introduction*. European Commission, Joint Research Centre of Ispra, Italy.

Sardesai, M. V. and Desai, A. K. (2013). "Investigation in to cable-structure interaction for extra-dosed bridge." *International Journal of Engineering Research and Applications* (IJERA), Vol. 3, No. 4, pp. 1424-1429, DOI: 10.1.1.410.5397.

Scanlan, R. H. (1977). " Motion of suspended bridge spans under gusty wind." *Journal of the Structural Division*, Vol. 103, No. 9, pp. 1867-1883, DOI: http://cedb.asce.org/CEDBsearch/record.jsp?dockey=0007611.

Selvam, R. P., Govindaswamy, S., and Bosch, H. (2001). *Aero-elastic analysis of bridge girder section using computer modeling.*, University of Arkansas, a report for Mack Blackwell Transportation Center, Arkansas, USA.

Shuxian, H. (2009). *Time domain buffeting analysis of Large Span cable-stayed bridge*, M.Sc. thesis. Norwegian University of Porto, Faculty of Engineering, Porto, Portugal.

Simiu, E. and Scanlan, R. (1996). *Wind effects on structures*, John Wiley & Sons, New York, 1996.

Soltane, S., Ben Mekki, O., Montassar, S., and Auricchio, F. (2010). "Damping stay cable transverse vibration using shape memory alloys and magneto rheological dampers." *Advances in Geomaterials and Structures*, Vol. 9, pp. 135-140, DOI: http://www-2.unipv.it/compmech/publications/2010_9p.pdf.

Soon Duck K. (2010). *Uncertainty of Bridge flutter velocity measured at wind tunnel tests*, The Fifth International Symposium on Computational Wind Engineering (CWE2010), Chapel Hill, North Carolina, USA. 23-27 May 2010.

Starossek, U. (1998). "Bridge instability in wind and spatial flutter analysis." *Invited lecture, Proceedings, Korean Society of Civil Engineers Annual Conference, Seoul, Korea*, Vol. 1, pp. 9-20, DOI: https://www.tuhh.de/sdb/starossek/Veroeffentlichungen/Dateien/finite%20element%20bridge%20flutter%20analysis%203.pdf.

Stærdahl, J. W., Sørensen Niels, N., and Nielsen, S. R. K. (2008). "Aeroelastic stability of suspension bridges using CFD." *Shell and spatial structures: Structural architecture - towards the future looking to the past.* Venice: University Iuav of Venice.

SudhirSastry, Y. B., Budarapu, P. R., Krishna, Y., and Devaraj, S. (2014). "Studies on ballistic impact of the composite panels." *Theoretical and Applied Fracture Mechanics*, Vol. 72, pp. 2-12, DOI: 10.1016/j.tafmec.2014.07.010.

SudhirSastry, Y. B., Budarapu, P. R., Madhavi, N., and Krishna, Y. (2015). "Buckling analysis of thin wall stiffened composite panels." *Computational Materials Science*, Vol. 96B, pp. 459-471, DOI: 10.1016/j.commatsci.2014.06.007.

Tan Van, V., Ho Yup, L., Nak Hyun, C., Seung-Taek, O., Young-Min, K., and Hak-Eun, L. (2011). " Flutter analysis of bridges through use of state space method." *Proceedings of the 8th International Conference on Structural Dynamics,* EURODYN 2011, Leuven, Belgium.

Thai, C. H., Ferreira, A. J. M., Bordas, S., Rabczuk, T., and Nguyen-Xuan, H. (2014). "Isogeometric analysis of laminated composite and sandwich plates using a new inverse trigonometric shear deformation theory." *European Journal of Mechanics - A/Solids*, Vol. 43, pp. 89-108, DOI: 10.1016/j.euromechsol.2013.09.001.

Thai, C. H., Nguyen-Xuan, H., Nguyen-Thanh, N., Le, T. H., Nguyen-Thoi, T., and Rabczuk, T. (2012). "Static, free vibration and buckling analysis of laminated composite Reissner-Mindlin plates using NURBS-based isogeometric approach." *International Journal for Numerical Methods in Engineering*, Vol. 91, No. 6, pp. 571-603, DOI: 10.1002/nme.4282.

Thai, H. C., Nguyen-Xuan, H., Bordas, S., Nguyen-Thanh, N., and Rabczuk, T. (2015). "Isogeometric analysis of laminated composite plates using the higher-order shear deformation theory." *Mechanics of Advanced Materials and Structures*, Vol. 22, No. 6, pp. 451-469, DOI: 10.1080/15376494.2013.779050.

Thiesemanna, L., Bergmann, D., and Starosseka, U. (2003). "Numerical and experimental evaluation of flutter derivatives by means of the forced vibration method." *Proceedings of the 11th ICWE, International Association for Wind Engineering*, Kanagawa, Japan, pp. 1571-1578.

Tong, C. (2010). "Self–validated variance–based methods for sensitivity analysis of model outputs." *Reliab. Eng. Syst. Safe*., Vol. 95, No. 3, pp. 301-309, DOI: 10.1016/j.ress.2009.10.003.

Ubertini, F. (2008). *Wind effects on bridges: Response, Stability and Control*. PhD thesis, University of Pavia, School of Civil Engineering, Pavia, Italy.

Valizadeh, N., Bazilevs, Y., Chen, J. S., and Rabczuk, T. (2015). "A coupled iga-meshfree discretization of arbitrary order of accuracy and without global geometry parameterization." *Computer Methods in Applied Mechanics and Engineering*, Vol. 293, pp. 20-37, DOI: 10.1016/j.cma.2015.04.002.

Valizadeh, N., Natarajan, S., Gonzalez-Estrada, O. A., Rabczuk, T., Tinh Quoc, B., and Bordas, S. P. A. (2013). "NURBS-based nite element analysis of functionally graded plates: Static bending, vibration, buckling and flutter." *Composite Structures*, Vol. 99, pp. 309-326, DOI: 10.1016/j.compstruct.2012.11.008.

Van Vu Tan, Lee, H. Y., Chun, N. H., Oh, S. T., Kim, Y. M., and Lee, H. E. (2011). "Flutter analysis of Bridges through use of state space method." *Proceedings of the 8th International Conference on Structural Dynamic*s, EURODYN 2011, Leuven, Belgium. 4-6 July 2011.

Vu Bac, N., Lahmer, T., Zhuang, X., Nguyen Thoi, T., and Rabczuk, T. (2016). "A software framework for probabilistic sensitivity analysis for computationally expensive models." *Advances in Engineering Software*, Vol. 100, pp. 19-31, DOI: 10.1016/j.advengsoft.2016.06.005.

Wilde, K. and Fujino, Y. (1998). "Aerodynamic control of bridge deck flutter by active surfaces." *J. Engrg. Mech.*, ASCE, Vol. 124, No. 7, pp. 718-727, DOI: 10.1061/(ASCE)0733-9399(1998)124:7(718).

Xavier. Ortiz, David Rival, and David Wood. (2015). "Forces and moments on flat plates of small aspect ratio with Application to PV wind loads and small wind turbine blades." *Joumal of Energies,* Vol. 8, pp. 2438-2453, DOI: 10.3390/en8042438.

Xiang, H. F., Ge, Y. J., and Zhu, L. D., etc. (2005). *Modern theory and Practice on Bridge Wind Resistance*, Beijing: China Communication Press.

Xiao, Y. Q., Hu, G., Tu, M. Q., and Zheng, R. Q. (2012). "The influence of turbulence integral scale to buffeting of long-span bridge." *Applied Mechanics and Materials*, Vols. 105-107, pp. 9-12, DOI: 10.4028/www.scientific.net/AMM.105-107.9.

Xie, X., Xiaozhang, Li, and Yonggang, S. (2014). " Static and dynamic characteristics of a long span cable stayed bridge with cfrp cables." *Materials*, Vol. 7, pp. 4854-4877, DOI: 10.3390/ma7064854.

Xie, J. and Xiang, H. (1985). "State-space method for 3-D flutter analysis of bridge structures." *Proc., Asia Pacific Symp. on Wind Engrg.*, India, pp. 269-276.

Xu, Y. L., Hu, L., and Kareem, A. (2014). "Conditional simulation of nonstationary fluctuating wind speeds for long-span bridges." *Journal of Engineering Mechanics*, Vol. 140, No. 1, pp. 61-73, DOI: 10.1061/(ASCE)EM.1943-7889.0000589.

Yang, S. W., Budarapu, P. R., Mahapatra, D. R., Bordas, S., Zi, G., and Rabczuk, T. (2015). " A meshless adaptive multiscale method for fracture." *Computational Materials Science*, Vol. 96B, pp. 382-395, DOI: 10.1016/j.commatsci.2014.08.054.

Yao-Jun, G. and Hai-Fan, X. (2008). "Bluff body aerodynamics application in challenging bridge span length." *BBAA VI International Colloquium on Bluff Bodies Aerodynamics and Applications.* Milano, Italy.

You-Lin, X. (2013). *Wind effects on cable supported bridges*, John Wiley & Sons Singapore Pte. Ltd.

Zhang, Z. Q., Ding, Y. L., and Geng, F. F. (2016). "Investigation of influence factors of wind-induced buffeting response of a six-tower cable-stayed bridge." *Shock and Vibration*, Vol. 2016, Article ID 6274985,16 p, DOI: 10.1155/2016/6274985.

Zhuang, X., Augarde, C., and Mathisen, K. (2012). "Fracture modelling using meshless methods and level sets in 3D: Framework and modelling." *International Journal for Numerical Methods in Engineering*, Vol. 92, pp. 969-998, DOI: 10.1002/nme.4365.

Zhuang, X., Huang, R., Rabczuk, T., and Liang, C. (2014). "A coupled thermo-hydro-mechanical model of jointed hard rock for compressed air energy storage." *Mathematical Problems in Engineering*, Vol. Article ID 179169, DOI: 10.1155/2014/179169.

Zi, G., Rabczuk, T., and Wall, W. A. (2007). "Extended meshfree methods without branch enrichment for cohesive cracks." *Computational Mechanics* Vol. 40, No. 2, pp. 367-382, DOI: 10.1007/s00466-006-0115-0.